Biochimica et Biophysica Acta, 509 (1978) 78—89
© Elsevier/North-Holland Biomedical Press

BBA 77994

DYNAMIC LIGHT SCATTERING CHARACTERIZATION OF THE DETERGENT-FREE, DELIPIDATED (Ca^{2+} + Mg^{2+})-ATPase FROM SARCOPLASMIC RETICULUM

Y. YEH [a], J.C. SELSER [a] and R.J. BASKIN [b]

[a] *Department of Applied Science and* [b] *Department of Zoology, University of California, Davis, Calif. 95616 (U.S.A.)*

(Received September 19th, 1977)

Summary

Dynamic light scattering studies have been conducted on the delipidated and detergent-removed (Ca^{2+} + Mg^{2+})-ATPase protein assemblies. Specific characterization of the state of aggregation and the extent of conformation change upon delipidation and detergent removal has been made. The results show that the prominent species are dimers and tetramers of very globular nature, with axial ratios of less than 2 : 1. The hydrodynamic radii of the dimers and the tetramers are, respectively, 57.5 Å and 74.5 Å.

The globular nature of these observed entities differ from the delipidated ATPase proteins recently obtained (LeMaire, M., Jorgensen, K.E., Roigaard-Petersen, H. and Moller, J.V. (1976) Biochemistry 15, 5805—5812). Present results suggest that upon the removal of detergents from the lipid-free ATPase protein assembly, only a rather limited degree of aggregation takes place. Such a condition is consistent with models of the membrane protein system which has limited regions of hydrophobic contact. Oligomeric assemblies with aqueous channels is a possible active Ca^{2+} transport model consistent with results of the present data, as well as the data from several other recent studies.

Introduction

The (Ca^{2+} + Mg^{2+})-ATPase protein assembly is the central element in the transport of calcium by the sarcoplasmic reticulum [1]. Essential to its functional ability is its complement of phospholipid molecules, particularly those in the phospholipid annulus surrounding the protein assembly [2]. Since delipidation results in the exposure of hydrophobic regions of the assembly, conformational changes occur. Extensive delipidation results in irreversible conformational change [3]. In the present study we examine the hydrodynamic configuration of delipidated, detergent-free (Ca^{2+} + Mg^{2+})-ATPase protein assemblies.

The work of Dutton and Singer [4] tends to rule out a rotating carrier mechanism for Ca^{2+} transport; at least one which involves rotation of the entire 119 000 protein. An alternative model involving a selective Ca^{2+} channel has been discussed [5,6]. Various lines of evidence have indicated the possibility of an oligomeric structure for the functional unit in sarcoplasmic reticulum membranes and, in particular, the possibility that the 80 Å intramembranous particles may represent an oligomer of the 119 000 (Ca^{2+} + Mg^{2+})-ATPase protein. Such an oligomeric structure could contain a selective ion channel.

Enzymatic activity has been retained in the detergent solubilized (Ca^{2+} + Mg^{2+})-ATPase enzyme [7]. Examination in an analytical ultracentrifuge resulted in estimates of protein monomer molecular weight of 119 000 ± 7000 and of Stokes radius of 50—55 Å. These results also indicated an asymmetric shape of delipidated monomer and dimer.

A detergent-free, delipidated preparation of (Ca^{2+} + Mg^{2+})-ATPase protein entities [3] showed optically clear solutions which contained 6.0-nm particles according to electron microscopy. Limited aggregation of the lipid-free molecule suggested an irreversible loss of hydrophobic surface following replacement of lipid by deoxycholate.

The present work extends these studies by further characterizing the lipid-free, detergent-free (Ca^{2+} + Mg^{2+})-ATPase protein assemblies. Our results, obtained using dynamic light scattering, indicate that dimers and tetramers are the prevalent species and that these are highly symmetrical. Hydrophobic shielding by limited aggregation is indicated by these results.

Materials and Methods

Sacroplasmic reticulum vesicles were obtained from rabbit psoas muscle according to the method of MacLennan [8]. Lipid-free, deoxycholate removed, ATPase protein entities were prepared according to Hardwicke and Green [3]. By this procedure, less than 1% of the detergent was reported to be remaining on the ATPase system.

Subsequent to this procedure, the sample was fractionated on a Sepharose 4B column without deoxycholate. The column, in a 10°C environment, was preequilibrated and eluted with 50 mM Tris · HCl/0.1 M KCl, pH 8. Absorbance scans were taken at 280 nm on consecutive fractions whose volumes varied between 2 and 4 ml. When the absorbance signal registered the presence of protein through the column, representative fractions of the elution peak were taken and prepared for further study by dynamic light scattering. In addition, protein concentrations on all dynamic light scattering samples were made by the modified Lowry method [9] after the light-scattering experiments were completed.

Those fractions taken for dynamic light scattering work from samples I and II were taken from the leading edge, the peak and the trailing edge of the absorbance vs. fraction curve (Fig. 1) while those from sample III straddled the peak and the sample IV fraction was taken from the peak. In this way it was assumed that the range of molecular weights and size fragments obtainable using the solubilization method would be covered.

The samples were filtered through a 0.22 μm Millipore filter in the filtered-

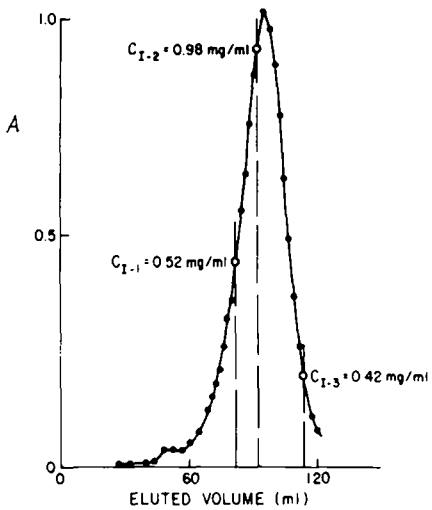

Fig. 1. Sample I absorbance (280 nm) vs. sample fraction eluted from the Sepharose 4B column. The three fractions examined by dynamic light-scattering are shown. Table I concentration data are based on the modified Lowry method [9].

air atmosphere of a laminar flow bench. Injection into cleaned and presealed light-scattering cells was made using 18 gauge stainless steel hypodermic needles attached downstream of the Millipore filtration unit. These samples were kept at 0°C until ready for the light-scattering experiments. Calcium transport capability and ATPase activity were determined for all samples using a pH method [10].

Light scattering experiments

All experiments were conducted at 20 ± 0.05°C. The 5145 Å line of an Ar^+ laser operating at about 100 mW in the TEM_{oo} mode was focused to a beam waist of approximately 25 μm inside the scattering cell, thereby defining the illuminated volume. Sample damage due to the intensity of the laser excitation was considered negligible based on the negative results of two checks: assuming that sample damage would have been accompanied by local heating within the illuminated volume resulting in changes in the local index of refraction, visual observation of changes in both the illuminated volume shape and the transmitted laser beam pattern were made. In the experiments reported here, no changes in either the illuminated volume shape or the transmitted beam profile were observed showing that there was no local heating and thus presumably no sample damage.

Collection of one coherence area of light scattered from the illuminated volume was insured by the use of a lens-diaphragm lens-pinhole system described previously [11]. The photon flux collected at a scattering angle of 90° was detected by an RCA 8850 photomultiplier tube with a type No. 116 photocathode. Photoelectric pulses were amplified and discriminated against noise by an SSR No. 1120 photon counting amplifier. Further pulse shaping was rendered by an Ortec No. 119 fast discriminator-shaper. The 'stretched'

25 ns pulses were thus compatible with the input requirements of the Malvern K-7023 digital correlator. Operating this instrument in the single-clip mode, the autocorrelation spectra of the detected pulses were computed and displayed simultaneously on a Tektronix Model No. 545 oscilloscope.

For any particular fraction under investigation, four experiments, each taking $3 \cdot 10^7$ parallel correlation samples, were conducted after allowing about 15 min for sample thermal equilibration. Since each experiment consumed about 100 s, each fraction studied remained at room temperature for a maximum of approximately 30 min. No changes in these spectra were observed during these 30 min periods, demonstrating that long term thermal degradation of samples was not a problem.

The dynamic light scattering experiments were recorded only if the sample fractions and their corresponding filtered buffer solutions met the 'dust' test, i.e., each fraction had to be free of any foreign scattering matter for the duration of an experiment. The typical solvent background count ranged from 2% of the sample count for the concentrated samples to almost 20% of the sample count for the low concentration fractions. However, correlation spectrum of this background was essentially flat revealing no interfering correlations from these background counts.

Before any spectral analysis was performed, the spectra were baseline corrected using the conventional theoretical expression for single clipping photon correlation analysis, (cf. ref. 12). To check the accuracy of this method of baseline calculation, benzene was used as a baseline 'calibration standard'. Because the density fluctuation dynamics of benzene occur on time scales much faster than those of the ATPase samples studied, benzene correlation spectra are flat at these slower times. Thus the benzene spectrum is, in effect, all baseline. At intensity levels comparable to those in the ATPase samples, it was found that the calculated benzene baselines and observed benzene baselines differed typically by less than 0.5% demonstrating that calculated baselines were sufficiently accurate to be used in correcting the dynamic light scattering spectra.

The resultant spectra were analyzed by two different schemes:

(1) Cumulant analysis. The method of cumulants developed by Koppel [13] was used to determine scatterer z-averaged diffusion coefficient, D_z, as well as the relative dispersions of these diffusion coefficients, δ_z.

In addition, the cumulant analysis used here was modified to check the data for either extreme heterogeneity or excessive intraparticle interference [11]. Any excess in either of these two quantities would render the dispersion analysis inaccurate. None of the experiments reported here were rejected for either of these reasons. Because δ_z is a direct measure of sample polydispersity. Accordingly, the large scattering angle of 90° was chosen to help eliminate the undesirable effect of dust particles on the spectrum.

(2) Multiple exponential fits. Since the cumulant analysis revealed large sample polydispersity and because it was expected that the autocorrelation spectra would result from sample distributions containing 'n-mers' of several kinds, it was decided that multiple exponential fits of the data should also be made. For these reasons, the spectra were analyzed by a weighted least-squares fitting of a linear combination of real exponential decay functions using the

Prony-Householder iteration method [14]. Generally, the data were amenable to double exponential fits with $\leqslant 10\%$ statistical errors on the individual diffusion coefficients, but with somewhat less accuracy (approx. 25%) in the determination of the correlation amplitudes. These results are consistent with other dynamic light scattering data analyzed in this manner (cf. ref. 15). In spite of errors of this magnitude, the relative amplitudes of the contributing protein fractions were discernible and helpful in the interpretation of the results.

Results

A. Cumulative expansion results

Table I is a compilation of all the data gathered on the delipidated ATPase system. The initial column indicates sample and fraction. The leading edge fraction is denoted by 1, the peak fractions by 2 and 3 and the trailing edge fraction by 4. Column 2 gives the best fit from the four spectra obtained for each sample. $\bar{D}_z$ and $\bar{\delta}_z$ are determined in the following way. The second order cumulant expansion yielded for each of the experiments values of D_z and δ_z, each with statistical fit uncertainties. Column 2 of Table I presents the averages of D_z and δ_z from experiments. These averages, $\bar{D}_z$ and $\bar{\delta}_z$, are presented as inverse variance weighted averages and simple averages, respectively, in order to better represent the variability in the results. Thus, in these tabulated data, both the experimented variation and the statistical fit variation for each sample have both been accounted for.

In examining the second column of Table I, it is seen that in moving from the leading edge fraction to the peak fraction and then to the trailing edge frac-

TABLE I

SAMPLE CONCENTRATION AND CUMULANT AND TWO-EXPONENTIAL FIT MEAN DIFFUSION COEFFICIENT ($\bar{D}_w^{20}$) RESULTS

Roman numerals specify the sample while arabic numerals specify the sample fraction.

Sample	Cumulant fit		Two-exponential fit		Concn. (mg/ml)
	$(\bar{D}_z \times 10^7)$ cm^2/s	$\bar{\delta}_z z$	$(\bar{D}_i \times 10^7)$ cm^2/s	$\frac{A_1}{A_2}$	
I-1	1.47	0.088	1.21 ± 0.08	$\frac{2}{1}$	0.52
			1.86 ± 0.19		
I-2	2.18	0.143	1.91 ± 0.02	$\frac{2}{1}$	0.98
			3.14 ± 0.11		
I-3	2.62	0.340	1.70 ± 0.11	$\frac{1}{1}$	0.42
			3.81 ± 0.33		
II-2	1.30	0.124	1.44 ± 0.03	$\frac{3}{1}$	0.49
			0.86 ± 0.07		
II-3	2.26	0.195	1.51 ± 0.03	$\frac{1}{1}$	0.75
			2.87 ± 0.05		
II-4	1.96	0.434	1.29 ± 0.06	$\frac{2}{1}$	0.28
			3.59 ± 0.28		
III-2	2.42	0.174	2.73 ± 0.07	$\frac{3}{1}$	0.32
			1.47 ± 0.07		
III-3	3.06	0.287	3.81 ± 0.28	$\frac{3}{2}$	0.22
			1.75 ± 0.16		
IV-2	2.33	0.30	1.85 ± 0.03		0.36

tion, $\bar{D}_z$ increases indicating a decrease in the average size of the scatterers. Correspondingly, the relative dispersion, $\bar{\delta}_z$, increases. These results seemed strange at first, since it was expected, on the basis of the studies of LeMaire, et al. [16], that trailing edge fractions would be mostly monomers. In fact, sample II-4, the fourth fraction of sample number II, exhibited a distinct decrease in $\bar{D}_z$ in conjunction with a rather large $\bar{\delta}_z$ suggesting that trailing-edge fractions actually contained both large and small protein assemblies. Consequently, it was decided that these data warrant another way of examination. Namely, perhaps the values do not reflect true polydispersity but instead represent the sum of a finite number of spectral components. Thus, multiple exponential fits of this spectrum, as well as all others, were made to distinguish between the different possible protein oligomers present in each sample.

B. Correlation spectra fit with finite number of exponentials

A program called EXPALS [14] was used to perform the multiple exponential fits to the data. The technique used is one developed by Householder. The method is basically an iterative one for finding amplitudes and decay constants. The program can initiate its search for these constants either with or without initial guesses. Even though the data of column 2 are available, in order not to bias the search, data fits were achieved using no initial guesses nor a priori weighting factors. All correlation data except the shot noise channel (zero time lag) were used. In Fig. 2 a typical baseline-corrected set of data is plotted in its semi-log format, principally to illustrate that the two exponentials found by this method fitted the data very well.

In all of the EXPALS analyses, the program was asked to fit three exponentials, with six undefined parameters. However, in all cases except one, only two exponentials could be found. Data in column 3 represent inverse variance weighted averages of all four experiments conducted with each sample. The sample IV-2 could only be fitted to a single exponential. Because of low sample concentration, the single exponent fit to this spectrum (in spite of the

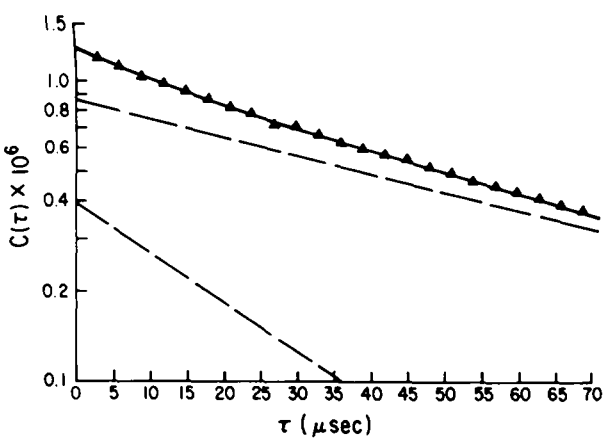

Fig. 2. Semi-logarithmic plot of the base-line corrected scattered light autocorrelation spectrum, $C(\tau)$, vs. elapsed time, τ, of fraction II-4. The distinctly non-linear character of this spectrum prompted analysis by both the cumulant expansion and double-exponential approaches. The two exponential components comprising the spectrum are shown as dashed straight lines.

large $\bar{\delta}_z$ calculated from the cumulant analysis) is considered to result from large variability in the spectrum so that the program could not reliably identify any other component. This variability could also then give rise to a large δ_z value from the cumulant analysis since δ_z is extracted from the coefficient of the quadratic term of the logarithm of the baseline corrected correlation spectrum and this coefficient is particularly difficult to measure when the correlation data are highly variable [11]. The general format of Column 3 lists both D_i values, $i = i,2$ and the ratio of the two computed amplitudes, A_i, for each experiment. Note that the $\bar{D}_z$ and $\bar{\delta}_z$ values are in good agreement with the two exponential fits. Typically, $\bar{D}_z$ is intermediate in value between the two-exponential fit $\bar{D}_i$ values. Consider, for example, the sample II-4 results. It is seen that the anomalous $\bar{D}_z$ value and the large $\bar{\delta}_z$ are both consistent with a two component exponential fit for which the stronger component exhibits a smaller $\bar{D}_i$ value. Moreover, the two $\bar{D}_i$ values are sufficiently different so that the curvature in the auto-correlation spectrum is quite obvious (Fig. 2). Accordingly, the $\bar{\delta}_z$ is large. Large $\bar{\delta}_z$ values were also observed for samples I-3 and III-3, both of which were trailing-edge fractions. Column 3 shows that these two samples have A_1/A_2 amplitude ratios either nearly unity or favoring the larger $\bar{D}_i$ component in spite in their disparate $\bar{D}_i$ values. As a result, $\bar{D}_z$ for these fractions were correspondingly larger.

Making further comparisons in the results, it is seen that the $\bar{D}_i$ values of Expts. I-1 and II-2 are relatively close to each other; accordingly $\bar{\delta}_z$ values from these experiments are small. Finally, note those samples exhibiting intermediate $\bar{\delta}_z$ values (I-2, II-3, III-2). The spectra from these fractions, when fitted to a two-exponential fit, gave somewhat lower values for the larger $\bar{D}_i$ while maintaining a smaller $\bar{D}_i$ component as well. It may have been that these samples contained more than two sizes of scatterer, but the statistical variance of the spectra was not low enough to warrant a three component interpretation.

Fig. 3 displays the groupings of the $\bar{D}_i$ values based on the double exponential fit results, all the values having first been corrected to aqueous solvent at 20°C. Note that there are three groups of data. The highest, with $\bar{D}_w^{20} = 3.73 \cdot 10^{-7}$ cm^2/s determined by weighting each $\bar{D}_i$ with the inverse of its

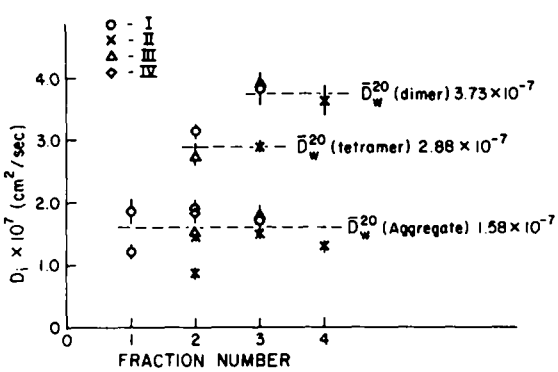

Fig. 3. Plot of $\bar{D}_w^{20}$ values versus fraction number for the four samples. The distinct $\bar{D}_w^{20}$ groups correspond to the association of the ATPase 'subunit' into dimers, tetramers and large aggregates.

variance, corresponded to an average Stokes-Einstein hydrodynamic radius of $<r_h>$ = 57.5 Å.

The second data group yields an average $\bar{D}_i$ of $2.88 \cdot 10^{-7}$ cm^2/s. The corresponding Stokes-Einstein hydrodynamic radius is $<r_h>$ = 74.5 Å.

The third, more heterogeneous grouping, results from larger scatterers and gives rise to the lowest diffusion coefficients. The average value of $\bar{D}_w^{20} = 1.58 \cdot 10^{-7}$ cm^2/s corresponds to an $<r_h>$ = 135.8 Å. This diffusion coefficient corresponds to a molecular weight of approx. $2 \cdot 10^6$ or about 17 ATPase subunits.

C. Depolarization factor for delipidated ATPase

Even though any of the detected particles rotates in aqueous solution at 20°C at a rate far too fast for the correlator instrumentation to detect its rate of rotational diffusion, the relative amount of depolarized light in the scattered signal was measured. With an intrinsic instrumental extinction factor of about $3 \cdot 10^{-5}$, it was found that of several samples measured, no sample gave counts distinctly above a noise level of about 200 counts per s. Accordingly, these particles were either quite spherical or there was very little molecular anisotropy per unit volume in delipidated ATPase. Since the chemical components found in ATPase are those found in other proteins which do depolarize light, it is concluded that the oligomers studied were globular. By contrast, depolarized light-scattering measurements made of comparable concentrations of native chicken ovotransferrin $M_r \sim 80\,000$ ($r_h \sim 50$ Å) using the same experimental apparatus measured a depolarized intensity that was almost 0.2% of the total scattered light. (Yeh, Y. (1977), unpublished data). The following comparison can be made: Wright [17] recently obtained rotational relaxation times for native human serum transferrin. Using the Perrin equations, this species could be treated as a prolate ellipsoid with an axial ratio of 2 : 1. Since it is well known that ovotransferrin and serum transferrin are similar in size and Fe^{3+} binding capacity, it seems reasonable to look at the consequences of using the same axial ratio for ovotransferrin. From this consideration, the ATPase results presented here suggest that the detergent- and lipid-removed ATPase entities probably have an axial ratio less than 2 : 1.

Discussion

Sample polydispersity

It is of interest to make some comparisons of the data presented here with the results of electron microscopy studies by Hardwicke and Green [3]. Since it is well known that quantitative size assessment of electron microscopically observed particles are subject to errors due to dehydration during fixation, caution must be exercised with respect to the validity of quantitative comparison. It is nonetheless possible to observe certain qualitative features of the 60 Å diameter and greater particles in the micrographs of Hardwicke and Green [3]. These particles were suggested to be either monomers, dimers or higher aggregates, with an overwhelming predominance for the smaller sizes. One may also comment on the observed heavy weighting to the larger sizes, as seen in column 4 of the dynamic light scattering data. Because light scattering intensities are proportional to C_iM_i, with C_i the mass of the ith species, and M_i

its corresponding molecular weight, the amplitude ratios from the double exponential fits are not a direct measure of the concentration of the various species. For example, Expt. II-4 gave an A_1/A_2 ratio of nearly 2 : 1 in favor of the larger species. However, since A_1/A_2 is reflective of the squares of the zero-time lag intensity correlation values, $(I_1/I_2)^2$, and since light scattering measures z-averages, [13] $I_i \propto C_i M_i$,

$$\frac{A_1}{A_2} = \left(\frac{C_1 M_1}{C_2 M_2}\right)^2 \tag{1}$$

If one makes the simplified approximation that these particles are solid spheres, then M_i is related to the translational diffusion coefficient, D_i, by $M_i \propto (D_i)^{-3}$. Under these approximations, one can estimate relative concentrations of the species when A_1/A_2, D_1, and D_2 are known:

$$\frac{C_1}{C_2} = \left(\frac{A_1}{A_2}\right)^{1/2} \left(\frac{D_1}{D_2}\right)^3 \tag{2}$$

For the sample considered, II-4, the A_1/A_2 ratio of 2 : 1 suggests that this experiment was sensitive to approx. 0.014 mg/ml of the larger aggregates.

Sample conformation

Since enzymatic activity is normally associated with proteins having very specific conformations and sites for activity, an inactive membrane protein has had its specific activation sites destroyed or shielded. For serum globular proteins found in aqueous environments, denaturation usually leads to more extended molecular conformation [18,19]. This is attributable to the breaking up of bonds necessary for stabilizing a specific site conformation by the denaturing agent, whether thermal or chemical. On the other hand, membrane proteins, upon delipidation and detergent removal, may denature in an entirely

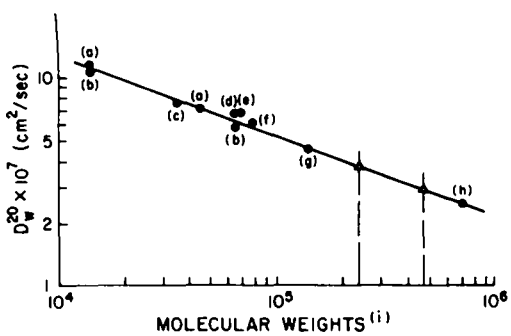

Fig. 4. Plot of D_w^{20} vs. molecular weight for a variety of globular proteins, as determined by other investigators using the dynamic light-scattering technique. A linear regression analysis of all points yielded $D_w^{20} \propto (M)^{-0.38}$. Assuming the smaller two ATPase entities observed in this study to be globular, their (△) respective molecular weights are 248 000 and 485 000. References cited: (a), Lysozyme, ovalbumin, [20]; (b) lysozyme, bovine serum albumin [21]; (c), β-lactoglobulin, [22]; (d), bovine serum albumin, [18]; (e), hemoglobin, [23]; (f), ovotransferrin, (Yeh, unpublished data); glyceraldehyde-phosphate dehydrogenase [24]; (h), ribosome 30 S, [25]; (i), molecular weights from Tanford, [26].

different way. The need to shield its hydrophobic portions from exposure to the aqueous environment may cause these denatured systems to contract so as to shield these hydrophobic regions and thereby acquire a more globular structure. On the basis of the results presented here, it seems reasonable to assert that delipidated ATPase acquires a globular conformation in an aqueous solution without detergent. In this case, it is expected that these globules would have a protein density very nearly that of those native globular proteins typically found in aqueous solutions. A comparison has been made of the D_w^{20} vs. molecular weight of naturally occurring globular proteins with those of the D_w^{20} values of the delipidated ATPase protein entities examined in this study. Fig. 4 is a compilation of the D_w^{20} data obtained exclusively from dynamic light scattering studies [18,20—25]. All of the tabulated proteins are globular in their native conformation, ranging in molecular weight from lysozyme ($M \approx$ 14 100) to ribosomes 30 s fragments with molecular weight of approx. 700 000. In this D_w^{20} vs. molecular weight plot, a linear regression analysis yielded, for an empirical equation of the form $D = K(M)^{-\alpha}$, a value of $\alpha \approx 0.38$. This is consistent with the globular nature of these systems since $M \propto V \propto r^3$ and so $D \propto 1/r \propto (M)^{-0.33}$. The results for the globular ATPase oligomers are included in the plot for comparisons.

It is clear that the observed species are not monomers. On the other hand, the resulting molecular weights of 245 000 and 485 000 for the two smaller ATPase species suggest that these were dimers and tetramers of the basic 119 000 molecular weight ATPase particle [27]. Results presented here provide evidence that delipidated detergent removed (Ca^{2+} + Mg^{2+})-ATPase shows little aggregation. In fact, the predominant species are dimers and tetramers. Such aggregation states reveal that these molecules must have a very limited hydrophobic surface which needs shielding from the aqueous solution.

The fact that monomer sizes were not observed in these studies indicates that the molecules probably aggregate via energetically most favorable paths. Instead of completely shielding its own hydrophobic region by extensive molecular rearrangement, two or four molecules can mutually shield their common hydrophobic regions without expending much energy in altering molecular conformations. On the other hand, the fact that these molecules do not seem to exhibit axial ratio asymmetry of as much as 2 : 1 seems to imply that the mutual hydrophobic shielding is taking place in a manner such that the monomer molecular asymmetry [7] is practically eliminated.

Comments

A reasonably consistent picture describing structural alteration of the (Ca^{2+} + Mg^{2+})-ATPase assembly can be drawn based on several works including the present study. One way to consider the 4 : 1 outside : inside particle ratio was to suggest that membrane protein ATPase oligomers are tetrameric units [28]. In order to identify the 4 : 1 ratio explicitly, however, the outer surface particles must be relatively far apart, each monomer thus preserving its monomeric identity. On the other hand, the inner surface can be thought of as having the 4 ends linked together via either hydrophobic or van der Waals interaction. Given the accepted dimensions of the sarcoplasmic reticulum membrane

bilayer thickness, those particles could be individually looked upon as elongated ellipsoids, $a : b \propto 6 : 1$ [7]. The transmembrane nature of this molecule is consistent with these sizes.

Upon delipidation the elongated ATPase molecules become predominantly monomers, but the shape is preserved via detergent-lipid protein complexing. It is also possible that glycerol protects the aqueous site of the protein so as to keep the protein active site in its native, functioning capacity. Le Maire et al.'s results [7] indicate that these entities have lower sedimentation coefficients, thus implying these particles are more elongated than inactive species. Correspondingly, the active ATPase molecules might be in the shape of the intact membrane constituents.

Upon further removal of detergent, the necessary conformation change is more dramatic. The dimers and tetramers, which are reported here, experience further conformation changes for hydrophobic shielding purposes.

The above picture of conformation change is also consistent with the idea that having achieved globular form, these molecules cannot easily be reactivated because of the rather strong shielding of the hydrophobic groups. In fact, several attempts to reinsert lipids into the ATPase dimers failed. (Baskin, R.J. and Deamer, D.W. (1977) unpublished data.)

Finally, it is important that these studies be followed by extensive studies of the reactivable ATPase. As reported by Dean and Tanford [29], such species are now achievable with only 4 mol of phospholipid/mol of protein if glycerol is present. A dynamic light-scattering study of such systems is being planned.

Acknowledgements

We thank R.J. Sylvester for preparing the delipidated ATPase samples used in this study and T.A. Hargreaves for helping to modify and then run the computer programs used in analyzing the resulting light scattering data. This work was supported in part by a grant from National Science Foundation PCM-73-06918 (to Y.Y. and J.C.S.) and by a grant from National Heart and Lung Institute, HL-12978 (to R.J.B.).

References

1 Baskin, R.J. (1977) in Membrane Proteins and Their Interactions with Lipids (Capaldi, R., ed.), Ch. 4, pp. 151—188, Marcel Dekker, Inc., New York
2 Green, N.M. (1975) Biochem. Soc. Trans. 3, 604—606
3 Hardwicke, P.M.D. and Green, N.M. (1974) Eur. J. Biochem. 42, 183—193
4 Dutton, A., Rees, E.D. and Singer, S.J. (1976) Proc. Natl. Acad. Sci. U.S. 73, 1532—1536
5 Singer, S.J. (1974) Annu. Rev. Biochem. 38, 805—833
6 Baskin, R.J. (1977) in Methodological Surveys in Biochemistry (Reid, E., ed.), Vol. 6, pp. 53—64, Horwood Ltd., Chichester
7 Le Maire, M., Jorgensen, K.E., Roigaard-Petersen, H. and Moller, J.V. (1976) Biochemistry 15, 5805—5812
8 MacLennan, D.H. (1974) in Methods in Enzymology (Fleischer, S. and Packer, L., eds.), Vol. 32, pp. 291—302, Academic Press, New York
9 Schacterle, G.R. and Pollack, R.L. (1973) Analyt. Biochem. 51, 654—655
10 Nishimura, J., Ito, T. and Chance, B. (1962) Biochim. Biophys. Acta 59, 177—182
11 Selser, J.C., Yeh, Y. and Baskin, R.J. (1976) Biophys. J. 16, 337—356
12 Oliver, C.J. (1973) in Photon Correlation and Light Beaming Spectroscopy (Cummins, H.Z. and Pike, E.R., eds.), pp. 151—228, Plenum Press, New York

13 Koppel, D.E. (1972) J. Chem. Phys. 57, 4814—4820
14 Gardner, C.D. (1970) UCRL No. 14541, Rev. 1
15 Chen, F.C., Chrzeszczyk, A. and Chu, B. (1977) J. Chem. Phys. 66, 2237—2238
16 Le Maire, M., Moller, J.V. and Tanford, C. (1976) Biochemistry 15, 2236—2342
17 Wright, A.K. (1976) J. Colloid and Interface Sci. 55, 109—115
18 McDonnell, M.E. and Jamieson, A.M. (1976) Biopolymers 15, 1283—1299
19 Nicoli, D.F. and Benedek, G.B. (1976) Biopolymers 15, 2421—2437
20 Dubin, S.B., Lunacek, J.H. and Benedek, G.B. (1967) Proc. Natl. Acad. Sci. U.S. 57, 1164—1171
21 Foord, R., Jakeman, E., Oliver, C.J., Pike, E.R., Blagrove, R.J., Wood, E. and Peacocke, A.R. (1970) Nature 227, 242—245
22 Chu, B., Yeh, A., Chen, F.C. and Weiner, B. (1975) Biopolymers 14, 93—117
23 Alpert, S.S. and Banks, G. (1976) Biophys. Chem. 4, 287—296
24 Gabler, R., Ford, N.C. and Westhead, E.W. (1975) Biophys. J. 15, 747—751
25 Gabler, R., Westhead, E.W. and Ford, N.C. (1974) Biophys. J. 14, 528—545
26 Tanford, C. (1961) Physical Chemistry of Macromolecules, p. 358, J. Wiley and Sons, Inc., New York
27 Rizzolo, L.J., Le Maire, M., Reynolds, J.A. and Tanford, C. (1976) Biochemistry 15, 3433—3437
28 Scales, D. and Inesi, G. (1976) Biophys. J. 16, 735—751
29 Dean, W.L. and Tanford, C. (1977) J. Biol. Chem. 252, 3551—3553